

ASSESSMENT OF THE PERFORMANCE OF AN HYPOLIMNETIC AERATOR EMPLOYING A WATER QUALITY MODEL

Arturo Palacio, Alejandro Rodríguez, Laura Martínez
Engineering Institute, National University Autonomous of Mexico
Apartado Postal 70-472, Coyoacan, 04510, Mexico, D.F.
email: vortex@vortex.iingen.unam.mx

ABSTRACT

A mathematical model which describes the thermohydraulic behaviour of a reservoir, is here presented and applied to assess the performance of an aerator of hypolimnetic type. This kind of equipment is designed to preserve the ecosystem while increasing the dissolved oxygen levels at the hypolimnion without major interaction with the water surface. The model developed to evaluate the water quality, takes into account the buoyancy effects into the turbulence model, considers the solar and atmospheric radiation as well as the evaporation, convection and long wave radiation terms for the heat balance, and solves two additional transport equations that consider the presence of the dissolved oxygen and the biochemical oxygen demand in the water. The results show a very good agreement with the design data provided by the equipment designers. The model may be used to establish operational policies of this (and other) kind of aerators.

Version: 2.1 HP750/UNIX 9.0

INTRODUCTION

The most common, obvious and persistent water quality problem is that of the so-called eutrophication (Mason [1991], Salas y Martino [1990]). Lakes and reservoirs deteriorate through excessive addition of plant nutrients, organic matter and silt, which combine to produce increased algae and rooted plant biomass, reduced water clarity, and usually decreased water volumes (Harper [1992]). In this condition water bodies lose much of their attractiveness for recreation, and their usefulness and safety as industrial and domestic water supplies. As a consequence water eutrophication can bring about economic losses in the forms of decreased property values, high cost treatments of raw drinking water, illness, depressed recreation industries, expenditures for management and restoration, and ultimately the need to build new reservoirs.

Management and restoration techniques are used to manipulate one or more internal chemical, biological, or physical processes or conditions in order to rehabilitate the water body (Ahl [1980], Vollenweider [1968], Jordan et al [1987], Cooke et al [1986]). In the strict sense, a reservoir can not be restored because it is by definition a human recent disturbance of a river, for which restoration would involve elimination of the dam among other steps; however, they can be restored to an earlier condition. Sediment removal, coupled with land management and the construction of devices to trap silt, would constitute a reservoir restoration and protection. Water bodies restoration is a relatively new and growing science and a proven "track record" for

some techniques is lacking; thus there is still much uncertainty in estimating the cost effectiveness of some techniques. For that reason a thorough prerestoration evaluation is an absolute requirement, not only for the increased assurance of success for the given water body, but also to contribute new knowledge that will benefit future project decisions.

The success of efforts to improve the quality of a water body depends on the thoroughness of the diagnosis prior to initiating restoration measures. This should contemplate a) the constituents and variables that should be determined in the watershed and its sediment; b) the sample number needed and their frequency; c) ways to express the data collected; d) levels of constituents that indicate trophic state; and e) how to determine the limiting nutrient. Restoration techniques are divided into four categories, based on their considered primary objective: 1) to control problems caused by algae; 2) to control excessive macrophyte biomass; 3) to remove sediment, and 4) to alleviate oxygen problems.

The lack of dissolved oxygen in some zones of the reservoir is the basic cause of water quality degradation, as it is fundamental for the correct performance of many aquatic organisms and for decomposition of the existing organic matter. Another factor that contributes to the decay of a water body is the increment of temperature, because the biological processes experiment an enhancement. For this reason, the problem intensifies during warm seasons when stratification takes place, because internal mixing is inhibited and therefore oxygen transport from superficial to lower zones is very scarce. In order to implement an adequate management or restoration program, it is required to know the performance of the reservoir along the year. In a very general form, a reservoir may be characterised according to two basic aspects: its morphology, which classify it as deep or shallow depending on its vertical dimensions, and the meteorological conditions. Schematically, figure 1 shows the typical behaviour expected in shallow and deep reservoirs during winter and summer, in terms of both temperature and dissolved oxygen profiles.

According to this figure, the stratification process occurs during the summer in deep reservoirs, and the interaction between the upper (epilimnion) and lower (hypolimnion) part of the reservoir is effectively inhibited by the thermocline (metalimnion); the epilimnion will experiment adequate levels of oxygenation due to the wind action, while the hypolimnion will tend to attain practically anoxic conditions. As expected, this problem is more dramatic in very warm regions, where the winter is not so severe as to cause complete mixing of the water. The evolution of the thermocline then determines in a way the water quality in terms of the dissolved oxygen concentration (Churchill & Nicholas [1967]). The factors that mainly determine the thermocline behaviour are the wind, the density currents, and the radiative and evaporative cooling of the surface (Alavian et al [1992], Imberger & Hamblin [1992]).

Among the restoration techniques, the aeration appears as the one which is gaining more popularity every day, the main reasons being the fact that it does not present noxious effects, and that its technologic development has allowed the reduction of

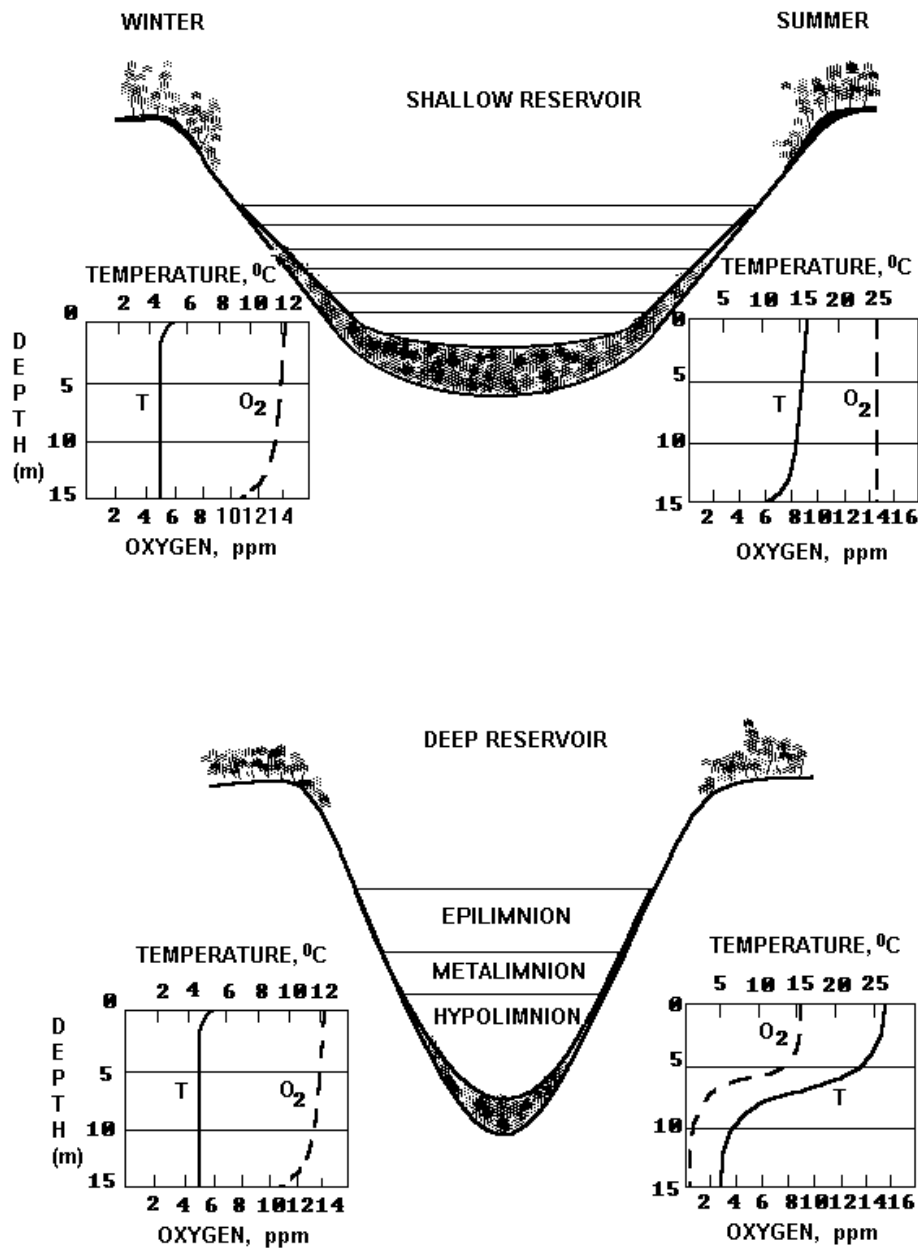


Fig. 1 Typical conditions of shallow and deep reservoirs.

costs up to levels which make feasible its use under a wide range of conditions. There are two types of aeration: mixing or destratification, and hypolimnetic. The first one is achieved by the use of pumps, water jets and air bubbles, and is mainly employed in the treatment of shallow water bodies (Fast et al [1976], Verner [1984]). The hypolimnetic aeration is a technique designed to counteract hypolimnetic anoxia and its associated problems (Ashley & Hall [1990]); its specific objectives are to raise the oxygen content of the hypolimnion without destratifying the water column or

warming the hypolimnion, and to provide an increased habitat and food supply for coldwater fish species.

Injection of air via air-lift systems has been the most popular for hypolimnetic aeration. Full air-lift brings bottom water to the surface by forcing compressed air into the bottom of an inner cylinder; the rising bubbles drive the air-water mixture to the surface exposing water to the atmosphere, and then returns it to the hypolimnion via an outer cylinder after first venting the air bubbles. Partial air-lift aerates hypolimnetic water in place, with water and air bubbles being separated at depth and the air discharged at the surface; it is probably the most frequently used system, possibly because of its great commercial availability, like the so called LIMNO aerator, Verner [1984] (figure 2). Procedures for sizing the hypolimnetic aerators to oxygenate hypolimnia without destratifying the water column have been outlined in detail by Lorenzen and Fast [1977], Ashley [1985], and Ashley et al [1987].

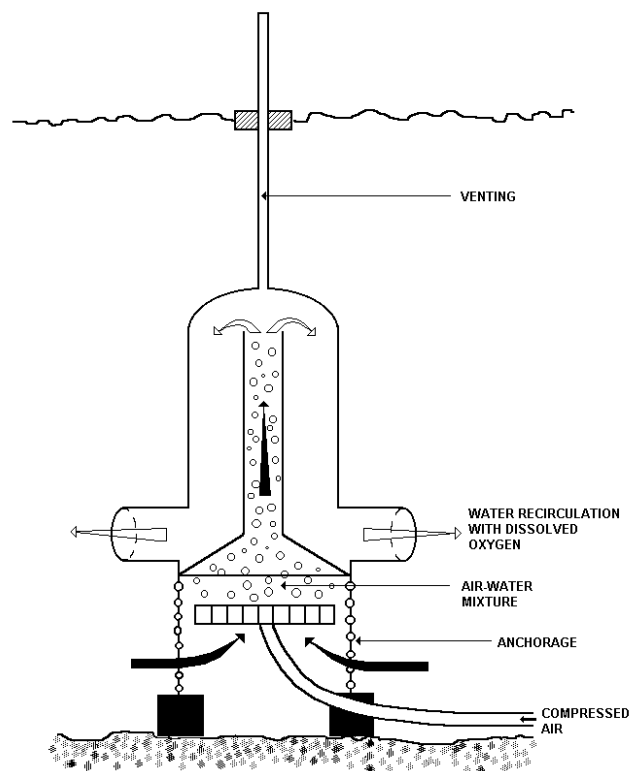


Fig. 2 Hypolimnetic aerator.

The reader interested in a more detailed description of restoration techniques, together with the costs associated with the use of several commercial equipments is referred to Martínez [1995].

PROBLEM DESCRIPTION

Considering that the main purpose of the simulation is to establish if the hypolimnetic aerator performs according to the designer specifications (figure 3), the reservoir is

assumed to be under completely unfavourable initial conditions, that is, anaerobic, without influents or effluents, and neglecting wind effects over the surface. The thermal stratification comprises the first 17 of depth, with a nine degrees gradient. This data corresponds to the experimental values observed in the reservoir of Zimapan.

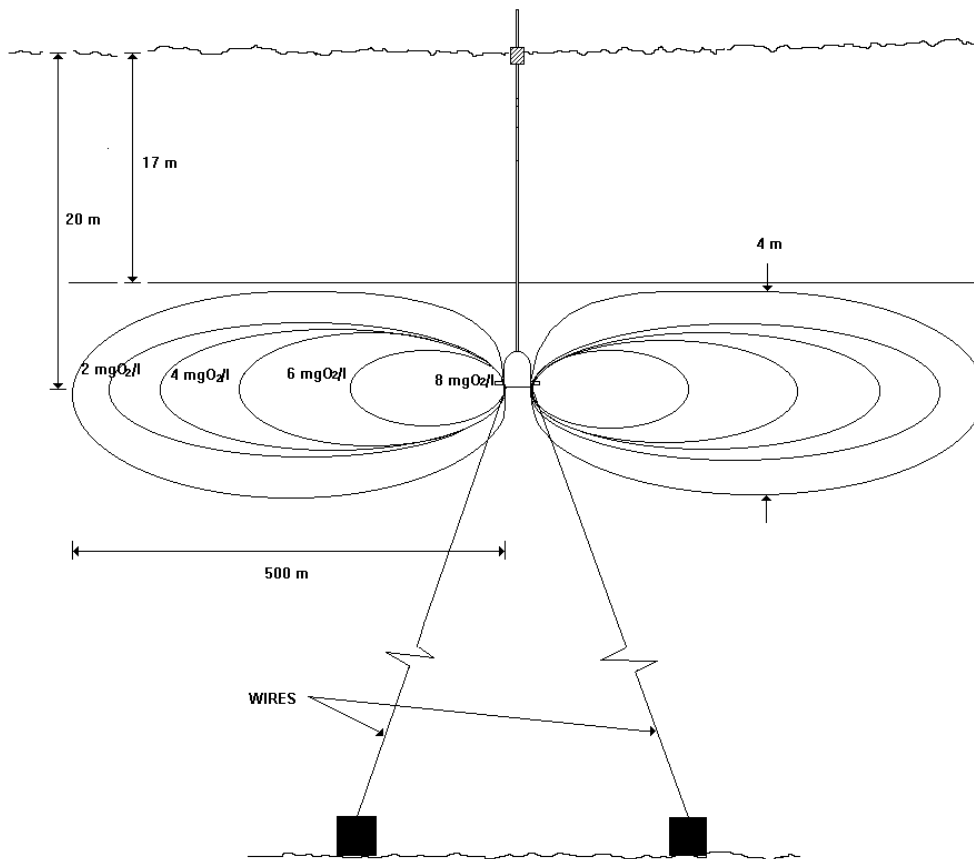


Fig. 3 Theoretical oxygen contours according to unit designer.

The LIMNO unit was represented with a deposit 4.6 m height and a radius of 1.2 m; the length of the exit pipes is 3 m. The aeration process takes place when compressed air is injected through the interior pipe of 0.7 m diameter, which forces the air-water mixture up and then returns the water to the hypolimnion via the outer cylinder. During the mixing process, oxygen is transferred to the water with a resulting concentration of 13 mg/l and then leaves the aerator at a rate of 61.6 l/s through each of six pipes of 0.5 m diameter. The aerator is assumed to be anchored at 60 m from the bottom of the reservoir whose average depth is 80 m.

Given the symmetry of the problem, it was simulated one sixth of the reservoir (1.047 rad) considering only one exit pipe of the aerator (fig 4). A polar system of coordinates was chosen to build a mesh which showed to be grid independent when assigned 9x40x35 cells in the x, y and z direction respectively, distributed in a non uniform way giving a total of 12600 nodes as shown in figure 5, where it can be

observed that the major density of cells takes place in the vicinity of the aerator discharge.

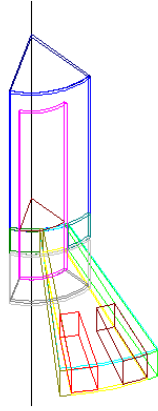


Fig. 4 Aerator representation.

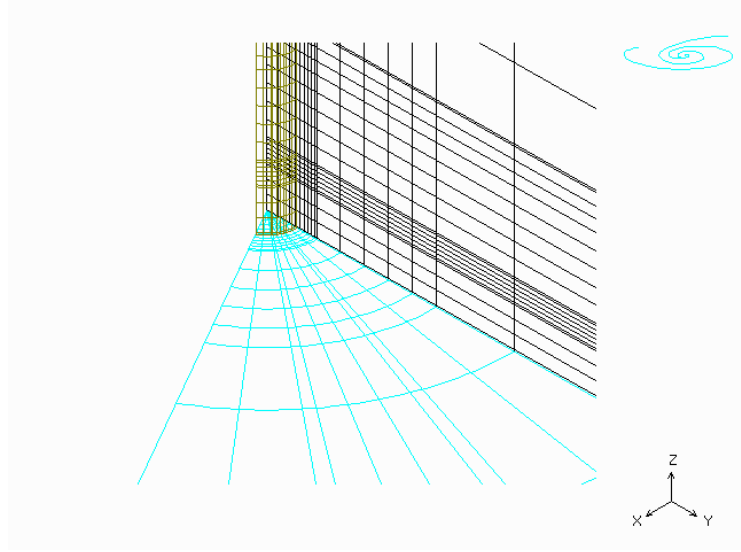


Fig. 5 Domain discretization.

Mathematical Formulation

The set of partial differential equations describing the problem examined herein, are those of continuity, momentum and energy, together with an additional couple of turbulence transport equations. This set of equations can be expressed in a general form as follows:

$$\frac{\partial}{\partial t} (\rho \phi) + \nabla \cdot (\rho \bar{V} \phi) = \nabla \cdot (\Gamma_{\phi} \nabla \phi) + S_{\phi} \quad (1)$$

where t denotes time, ϕ represents any dependent variable, V the velocity vector, ρ the fluid density, Γ the transport coefficient of the dependent variable, S the source of ϕ per unit volume and ∇ is the vector differential operator.

The dependent variables and their corresponding transport equations, are listed below in Table 1, where u, v, w are the velocity components in the coordinates directions x, y and z respectively, T is the temperature, which is directly calculated from the energy equation, C represents the concentration of dissolved oxygen, k is the turbulent kinetic energy and ε its dissipation rate; μ_l is the laminar dynamic viscosity, μ_t the turbulent viscosity, and μ_e the effective viscosity; D is the diffusion coefficient of oxygen in water, σ_k and σ_ε are the standard turbulence-model coefficients which will be described later.

The source term for the momentum equation is given by:

$$S_m = - \nabla p + \rho \underline{g} + \nabla \cdot \left[\mu_e (\nabla \underline{U})^T - \frac{2}{3} (\mu_e \nabla \cdot \underline{U}) I \right] \quad (2)$$

where p is static pressure, \mathbf{g} gravity vector, I the unit tensor, and the superscript T denotes the transpose of the dyadic.

TABLE 1. Transport coefficients for variable ϕ

	ϕ	Γ_ϕ
Continuity	1	0
Momentum	u, v, w	μ_e
Temperature	T	$(\mu_l / \sigma_l + \mu_t / \sigma_T)$
Concentration	C	D
Turbulent kinetic energy	k	$(\mu_l + \mu_t / \sigma_k)$
Dissipation rate of k	ε	$(\mu_l + \mu_t / \sigma_\varepsilon)$

For the energy equation a source term considering the temperature variation due to the temporal pressure changes is included:

$$S_T = \frac{I}{c_p} P_n \quad (3)$$

where C_p is the specific heat capacity of the water at constant pressure. Regarding the transport equation for dissolved oxygen (DO), this equation must always be coupled with the one corresponding to the biochemical oxygen demand (BOD). In order to avoid spending unnecessary computational time, for the present calculations no source terms have been considered for DO, and as a boundary condition it has been assumed that far from the aerator the concentration of DO is zero; this allows to include the additional transport equation for BOD. However, the reader interested in analysing the full set of equations corresponding to the interaction of DO and BOD is referred to Palacio et al [1994], where they have been applied to the case of Zimapan reservoir in Mexico.

Turbulence model

The turbulence model employed is the standard k - ε model, where the kinetic energy k , and its dissipation rate ε , represent the velocity and length scale of the turbulent motion respectively. The corresponding source terms are:

$$S_k = (P_k - \rho \varepsilon + G_B) \quad (4)$$

$$S_\varepsilon = \left(C_{1\varepsilon} P_k - C_{2\varepsilon} \rho \varepsilon + C_{3\varepsilon} G_B \right) \frac{\varepsilon}{k} \quad (5)$$

where P_k is the production rate of k , and G_B is the production or destruction of k due to buoyancy effects; these two terms may be written as:

$$P_k = \mu_t \left[\nabla \underline{U} : (\nabla \underline{U} + (\nabla \underline{U})^T) \right] \quad (6)$$

$$G_B = - \frac{\mu_t}{\rho \sigma_t} \underline{g} \cdot \nabla \rho \quad (7)$$

The turbulent viscosity is calculated from the local values of \mathbf{k} and ε as follows:

$$\mu_t = C_\mu \rho k^2 / \varepsilon \quad (8)$$

The values assigned to the turbulent constants are the standard ones recommended by Launder and Spalding [1974]:

$$C_\mu=0.09; C_{1\varepsilon}=1.44; C_{2\varepsilon}=1.92; C_{3\varepsilon}=1.0; \sigma_k=1.0; \sigma_\varepsilon=1.314 \quad (9)$$

Boundary Conditions

The model takes into account the friction effect at the bottom of the reservoir, while for the free surface the wind effect as well as heat exchange may be activated. At the bottom, the wall-function approach outlined by Rodi [1980] is adopted, which means that the boundary conditions are not specified right at the wall but at a point outside the viscous sublayer, where the logarithmic law of the wall prevails and the turbulence can be assumed in local equilibrium. At the free surface the wind effect may be considered through a shear stress:

$$\tau = C_d \rho_a U_{10}^2 \quad (10)$$

where $C_d \approx 0.9E-03$ is the drag coefficient, ρ_a is the air density, and U_{10} is the wind velocity at 10 m height.

The heat transfer mechanisms considered between the water body and the surroundings are the solar and atmospheric radiation in what refers to heat gain, and evaporation, convection and long wave radiation in respect of heat losses. According to this, the net heat flow may be calculated with the following expression, Harleman [1982]:

$$Q_{net} = Q_{sol} + Q_{atm} - (Q_{br} + Q_{ev} + Q_c) \quad (11)$$

where Q_{sol} is the solar radiation heat flow, Q_{atm} considers the radiation from the atmosphere, Q_{br} is the long wave radiation from water into air, Q_{ev} is the evaporative heat flow, and Q_c is the heat flow by convection. The solar radiation heat flow may be calculated from:

$$Q_{sol} = (1 - \beta) \phi_0 e^{-\eta y} + \beta \phi_0 \quad (12)$$

where ϕ_0 is the incident total solar radiation per unit area, η is the extinction factor which depends on turbidity of the water, y is the water column depth, and β is the energy fraction absorbed by the water surface. The atmospheric radiation (long wave) is given by:

$$Q_{atm} = \{ C_1 + C_2 T_{air} \} (1 + 0.17 C_{ld}^2) \quad (13)$$

where C_{ld} is the cloudiness coefficient, $C_1 = 208.733$, $C_2 = 6.2363$ and T_{air} is the air temperature. The heat flow from the water to the air due to long wave radiation is obtained from the next equation (Ryan & Harleman [1974]):

$$Q_{br} = a + b T_{sup} \quad (14)$$

where a and b are constants with values 308.2 and 4.9 respectively, and T_{sup} is the superficial water temperature. Heat losses by evaporation may be calculated by the expression (Adams [1990]):

$$Q_{ev} = \{ Q_{free}^2 + Q_{forc}^2 \}^{1/2} (P_{sup} - P_{air}) \quad (15)$$

where P_{sup} is the partial pressure of water vapour at the surface, P_{air} is the partial pressure of water vapour in the air at 2 m above the surface, Q_{free} is the term which takes into account the temperature difference between the water surface and the air, calculated from (Adams [1990]):

$$Q_{free} = 2.7 (T_{sv} - T_{av})^{1/3} \quad (16)$$

Q_{forc} is a term that includes the wind effects through the relation:

$$Q_{forc} = 3.2 V_{air} \quad (17)$$

In equation (16) T_{sv} and T_{av} are the so called saturation and ambient virtual temperatures respectively which are determined from the absolute temperature θ_v using the following equations:

$$T_{sv} = \theta_v - 273.15$$

$$\theta_v = (T_{sup} + 273.15) (1 + 0.61 w) \quad (18)$$

$$w = 0.622 \frac{P_{vap}}{P_{bar} - P_{vap}}$$

where w is the specific humidity, P_{vap} is the partial pressure of water vapour and P_{bar} is the barometric pressure. To calculate the partial pressure of the water vapour, the relative humidity ϕ is involved through:

$$P_{\text{vap}} = \phi P_{\text{sup}}$$

For the ambient virtual temperature, the same set of equations (18) is employed considering air conditions at 2 m above the surface. The convective heat flow is given by (Ryan & Harleman [1974]):

$$Q_c = Q_{ev} R_b \quad (19)$$

where R_b is Bowen relation:

$$R_b = C \left\{ \frac{T_{sup} - T_{air}}{P_{sup} - P_{air}} \right\} \quad (20)$$

For the calculations, the ambient temperature and solar radiation variations along the day are considered through sinusoidal functions with hourly averages. The solution algorithm is based upon the well-known iterative “guess-and-correct” procedure of Patankar and Spalding [1972], but modified according to the SIMPLEST algorithm of Spalding [1982].

PRESENTATION AND DISCUSSION OF RESULTS

The model was run covering a period of one month, as it was observed that after approximately 23 days it reached practically stable operational conditions, which coincides with the 20 to 30 day interval prescribed by the designer. The typical velocity distribution within the aerator is shown in figure 6, where it can be seen

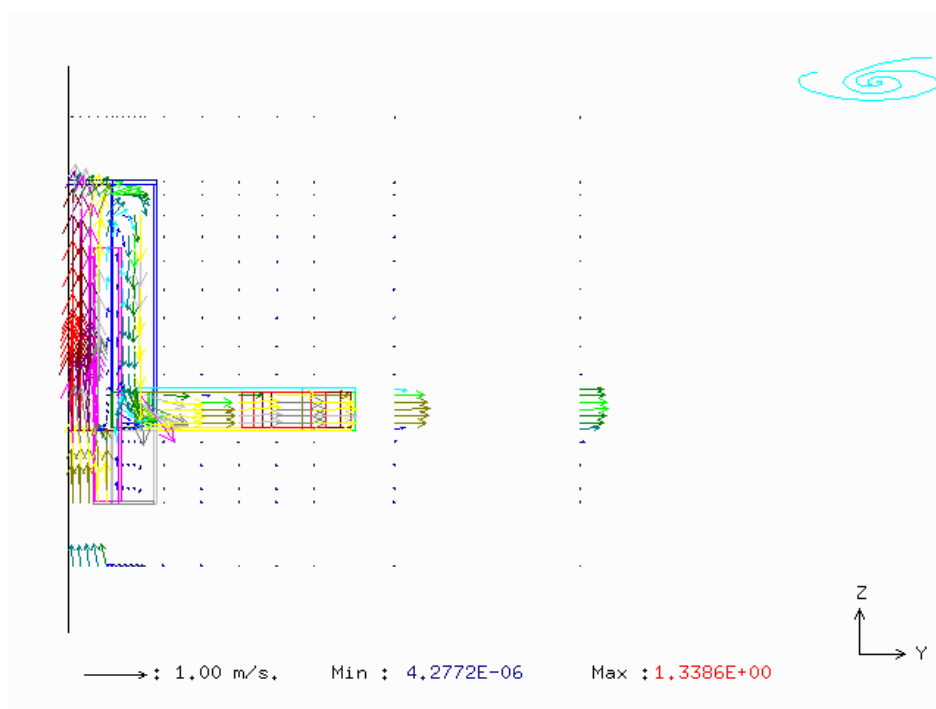


Fig. 6 Flow patterns inside and in the vicinity of the aerator.

that the maximum velocity of 1.3 m/s corresponds to the centre line of the prescribed parabolic profile, which was calculated to attain the correct mass flow rate. The density of the mesh in the aerator was enough to reproduce small recirculation zones due to the wall friction and the geometry itself. The same figure reveals several aspects that were expected, like the preservation of the parabolic profile at the exit of the pipe, which rapidly mixes with the surrounding water exchanging momentum, losing its shape and creating additional recirculation zones in the vicinity of the pipe due to the drag of the adjacent layers of water. The thermal stratification was practically preserved during calculations, as changes smaller than 2 °C were observed. Figures 7 to 13 show contours of the evolution of the dissolved oxygen. Due to the extensive amount of information generated, there were chosen only those times for which relevant changes on the oxygen patterns take place inside the reservoir during the aerator operation. Additionally to the coloured scale which indicates in blue and red the minimum and maximum values of oxygen concentration respectively, there have been included specific isocontours in white in order to clearly show the magnitude and extent of the dissolved oxygen in mg/l. Figure 7 corresponds to conditions after 6 hours of operation of the aerator; it has been magnified in the vicinity of the discharge as the influence area is still very reduced. The approximate maximum extent of the plume of oxygen is indicated by the isocontour corresponding to 1 mg/l. The shape of the contours is very close to the symmetric curves prescribed by the manufacturer (figure 3).

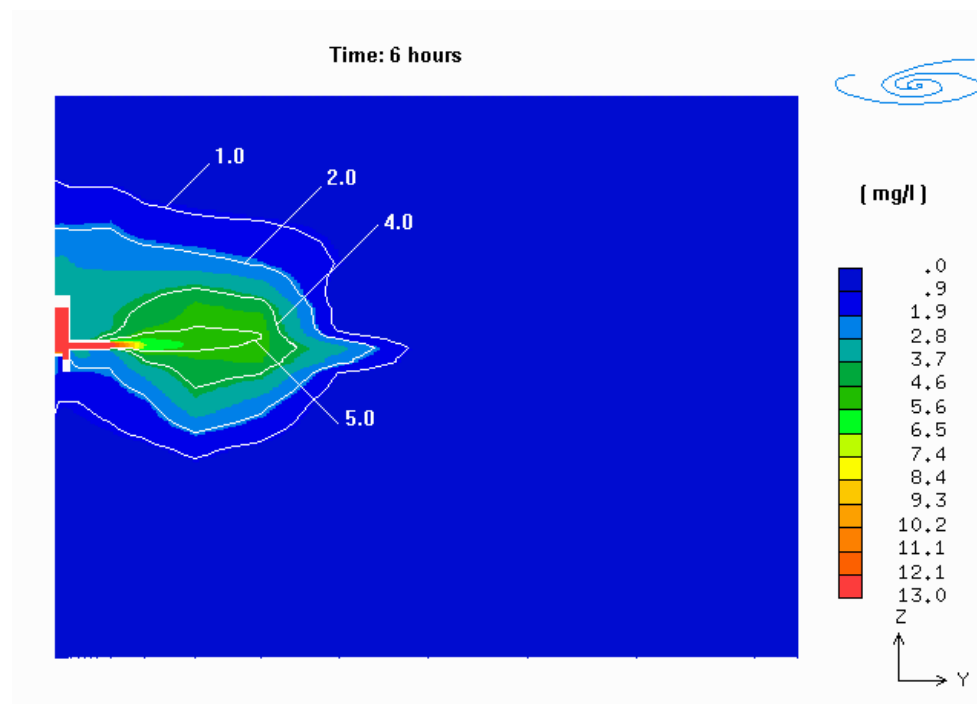


Fig. 7 Oxygen isopleths after 6 hours of the aerator's operation.

The rest of the figures are presented using a modified vertical scale with a factor of two; this allows a better appreciation of the area affected by the aerator. The symmetry of the contours starts to disappear after two days (fig. 8), and from that time on the curves show a very marked elongation, which coincides with the fact that after 48 hours the flow patterns have reached a quasi-stable condition, establishing a

well defined zone of approximately 5 m of width that confines the plume in its upper and lower portion, as illustrated in figure 9 after 3 days.

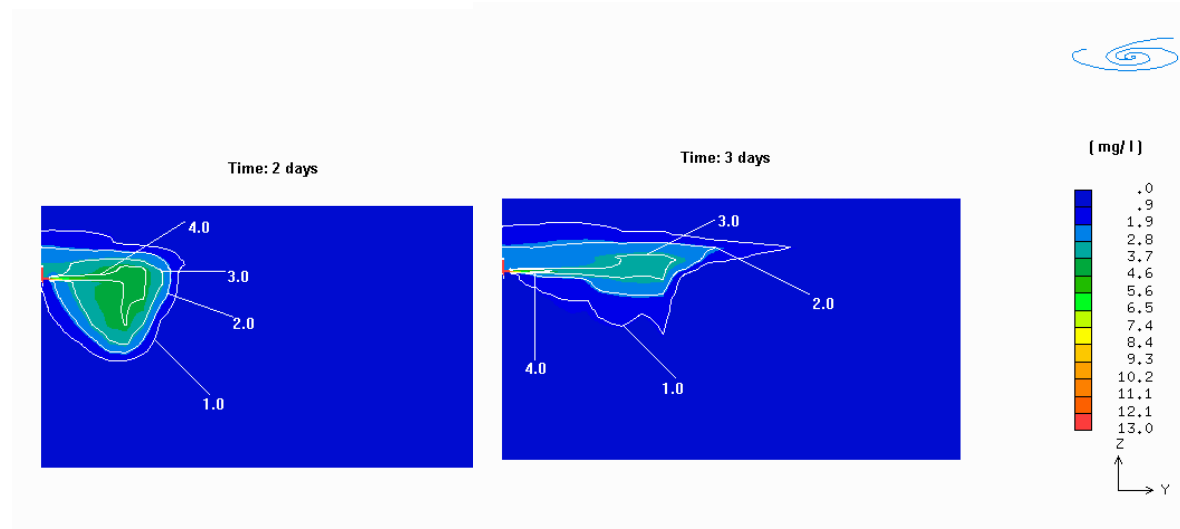


Fig. 8 Oxygen isopleths after 2 days of the aerator's operation.

Fig. 9 Oxygen isopleths after 3 days of the aerator's operation.

Wind effects are likely to modify these patterns in the upper region where additional reaeration is then expected.

After one week of operation, figure 10 indicates that a value of 2 mg/l appears as a limiting value above which the plume keeps a well-defined boundary. Two weeks later the contour corresponding to 1 mg/l provides the boundary of the plume (fig. 11), which reaches a practically stable condition after 23 days of operation of the aerator as illustrated in figure 12.

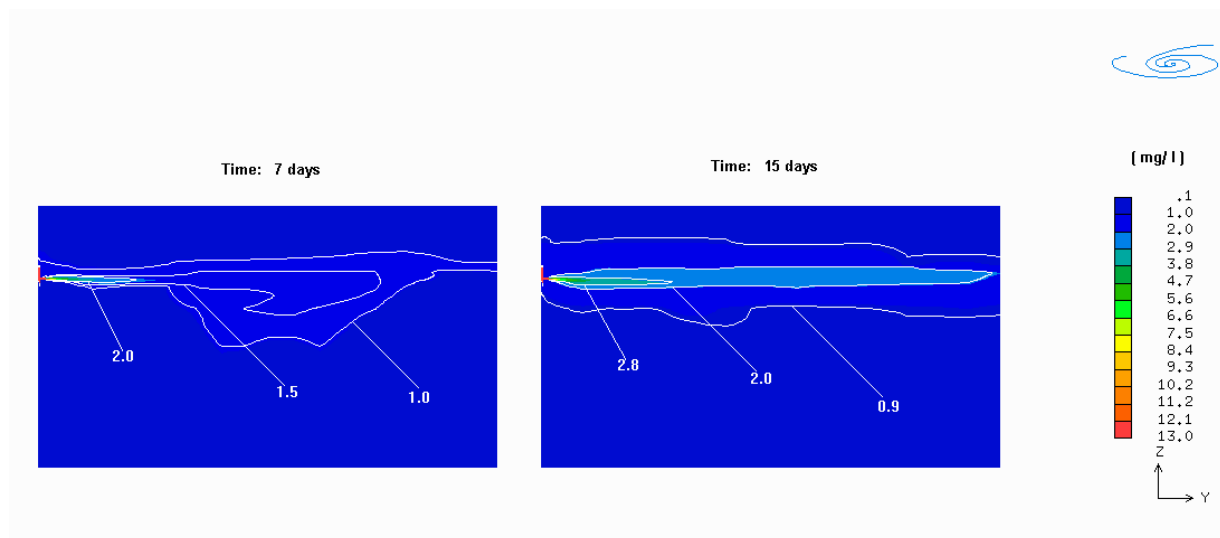


Fig. 10 Oxygen isopleths after 7 days of the aerator's operation.

Fig. 11 Oxygen isopleths after 15 days of the aerator's operation.

Finally, figure 13 confirms that after one month of operation of the aeration unit, the oxygen contours reached seven days before remain basically the same.

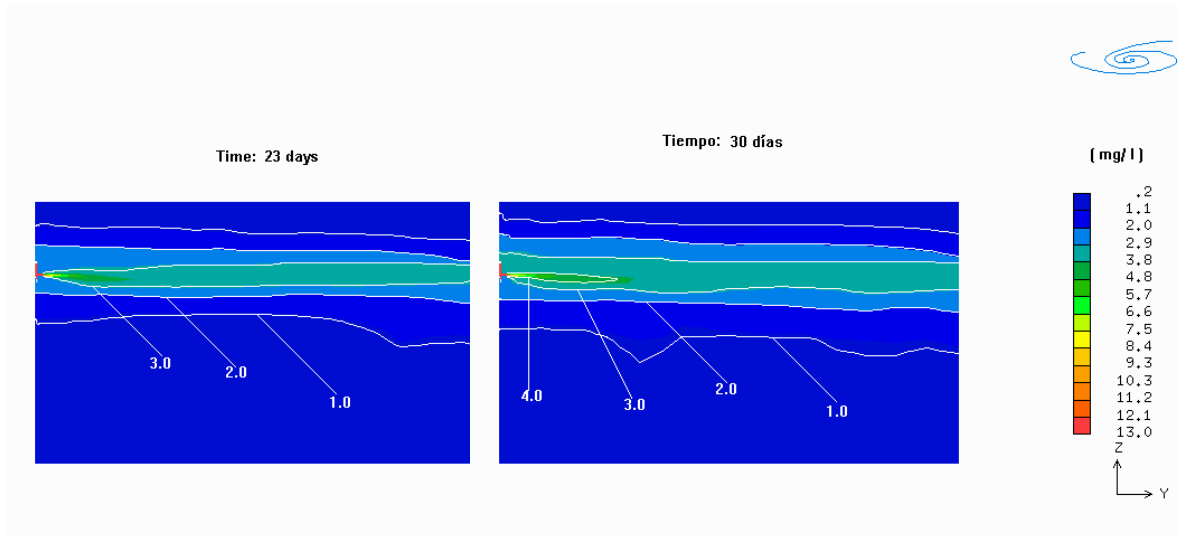


Fig. 12 Oxygen isopleths after 23 days of the aerator's operation.

Fig. 13 Oxygen isopleths after 1 month of the aerator's operation.

It can be observed that the final shape of the isopleths appears more elongated than the ones prescribed by the designer.

CONCLUSIONS AND RECOMMENDATIONS

A mathematical model developed to evaluate the quality of water bodies, was applied to assess the performance of an hypolimnetic aerator in the Zimapán reservoir, in Mexico. For the established initial conditions of the reservoir, as well as the geometric and operational specifications of the aerating unit, it was necessary a simulation time of nearly one month to attain stable conditions in terms of the oxygen isopleths within the reservoir. Even though the comparison with the design data provided by the equipment designers is more qualitative, the results show a very good agreement. attending to three aspects: the level of oxygenation of the water, the time necessary to reach stable conditions, and the shape of the isopleths. It is clear that the model may be used to establish operational policies of this kind of aerators, as well as to study alternative restoration techniques.

REFERENCES

- Adams E E, Cosler D J, Helfrich K R (1990), "Evaporation From Heat Water Bodies: Predicting Combined Forced Plus Free Convection", *Water Resources Research*, 26: 425-435.
- Ahl, T (1980), "Eutrophication in relation to the load of pollution". *Water Technology* 12(2). International Association on Water Pollution Research Proceedings of a Seminar on Eutrophication of Deep Lakes. Persimmon Press, Gjøves, Norway, (Jun 19-20, 1978), Great Britain: pp 4961.

- Alavin, V., G H Korla, R A Denton, M C Johnson y H G Stefan (1992), "Density currents entering lakes and reservoirs", ASCE J Hydr Eng 118(11) 1464-1489.
- Ashley, K (1983), "Hypolimnetic aeration of a naturally eutrophic lake: physical and chemical effects", Can J Fish Aquat Sci vol 40.
- Cooke, G D, Welch, E B, Peterson, S A y Newroth, P R (1986), "Lake and reservoir restoration", Butterworths, Massachusetts.
- Churchill, M A y W R, Nicholas (1967), "Effects of impoundment's on water quality", ASCE J of the Sanit Eng Div 93 (6): 73-90.
- Fast, A W, Lorenzen, M W y Glenn, J H (1976), "Comparative study with costs of hypolimnetic aeration", J Environ Eng Div ASCE 1026:1175-1187.
- Harleman, D R F (1982), "Hydrothermal analysis of lakes and reservoirs", ASCE J Hydr Div 108 (3): 302-325.
- Harper, D (1992), "Eutrophication of Freshwaters", Chapman & Hall, Londres: 321.
- Imberger, J y P F, Hamblin (1992), "Dynamics of lakes, reservoirs and cooling ponds", Ann Rev Fluid Mechanics, 14 153-187.
- Jordan, W R, Gilpin, M E, Ober, J D, Eds (1987), "Restoration Ecology: A synthetic Approach to Ecological Research", Cambridge University Press, Nueva York.
- Launder, B E y D B, Spalding (1974), "The Numerical Computation of Turbulent Flow", Comp Meth Appl Mech Eng 269-289.
- Martinez, L E (1995), Métodos para Oxigenación de Embalses de Centrales Hidroeléctricas, BSc Thesis, Faculty of Engineering, National University Autonomous of México.
- Mason, C F (1991), "Biology of Freshwater Pollution", Longman Scientific & Technical, Nueva York, 2ª de, pp 95'138.
- Palacio, A Rodríguez, A Mazari, M, *et al* (1994), "Evolución de la Calidad del Agua del Embalse del P.H. Zimapan, Hidalgo", Instituto de Ingeniería, UNAM, informe elaborado para CFE, II3127.
- Rodi W (1993), "Turbulence models an their Application in Hydraulics. A state-of-the-art review", 3rd De IAHR Monograph, Balkema, Rotterdam NL.
- Ryan P J Harleman D R F (1974), "Surface Heat Loss From Cooling Ponds", Stolzenbach, K D, Water Resources Research.
- Salas H J y P Martino (1990) "Metodologías Simplificadas para Evaluación de Eutroficación en Lagos Cálidos Tropicales 1981-1990", Programa Regional Centro Panamericano de Ingeniería Sanitaria y Ciencias del Ambiente, Organización Mundial de la Salud, Organización Panamericana de la Salud, Lima, Perú: 51.
- Verner, B (1984), "Long-term effect of hypolimnetic aeration of lakes and reservoirs with special consideration of drinking water quality and preparing cost"" EPA-440/5-84-001, pp 134-138.
- Vollenweider, R A (1968), "Water Management Research, Scientific Fundamentals of the Eutrophication of Lakes and Flowing Waters, with particular reference to Nitrogen and Phosphorus as factors in Eutrophication", OECD, Paris Technical Report DAS/CS1/68.

Q1 and GROUND Listing

```
TALK=f;RUN( 1, 1);VDU=TTY
IRUNN = 1;LIBREF = 0
  GROUP 1. Run Title
TEXT(Difusion de Oxigeno en un Embalse      )
  ***
rg(99)=1.0/4186.0
BOOLEAN(TAHOE)
REAL(NETFLU,CNET1,CNET2,CLD,TAIRE,PATM,FISUP,FI2M,W2M,ALFA)
  ***                                     *****
  ***** Constantes del NET ATMOSPHERE RADIATION          *****
CNET1=208.733;CNET2=6.2363;CLD=0.05;TAIRE=20.0
NETFLU=(CNET1+CNET2*TAIRE)*(1.0+0.17*CLD**2.0)*RG(99)
***** Constantes del short wave SOLAR RADIATION          *****
  * RG(1)=eta;RG(2)=beta;RG(3)=FI(radiacion)
rg(3)=500.0
TAHOE=f
IF(TAHOE) THEN
rg(1)=0.05;rg(2)=0.4
ELSE
rg(1)=0.75;rg(2)=0.5
ENDIF
***** Constantes del long wave BACK RADIATION            *****
rg(4)=308.2;rg(5)=4.9
***** Constantes de perdidas por EVAPORACION            *****
FISUP=1.0;FI2M=0.2;W2M=5.0;ALFA=1.0E+03;PATM=900.0
rg(6)=FISUP;rg(7)=FI2M;rg(8)=PATM;rg(9)=W2M
rg(10)=48.931;rg(11)=-6833.96;rg(12)=-5.169;rg(13)=ALFA
rg(14)=TAIRE
*****
  GROUP 2. Transience; time-step specification
STEADY=f;GRDPWR(T,30*12.-282.,86400.*31.,1.0)
tfirst=86400. + 564*3600.
*****
  Groups 3, 4, 5 Grid Information
  * Overall number of cells, RSET(M,NX,NY,NZ,tolerance)
RSET(M,9,40,35)
  * Overall domain extent, RSET(D,name,XULAST,YVLAST,ZWLAST)
RSET(D,CHAM,1.047E+00,3.000E+02,8.000E+01)
  * Set objects: name  x0          y0          z0
  *                   dx          dy          dz
RSET(B,B1, .000E+00, .000E+00, .000E+00,
1.047E+00, 0.700E+00, 8.000E+01)
RSET(B,B2, .000E+00, .000E+00, .000E+00,
1.047E+00, 0.750E+00, 8.000E+01)
RSET(B,B3, .000E+00, .000E+00, .000E+00,
1.047E+00, 1.200E+00, 8.000E+01)
RSET(B,B4, .000E+00, .000E+00, .000E+00,
1.047E+00, 1.250E+00, 8.000E+01)
RSET(B,B5, .000E+00, .000E+00, .000E+00,
1.047E+00, 4.250E+00, 8.000E+01)
RSET(B,B6, .000E+00, .000E+00, .000E+00,
```

```

1.047E+00, 3.000E+02, 5.540E+01)
RSET (B,B7, .000E+00, .000E+00, .000E+00,
1.047E+00, 3.000E+02, 5.545E+01)
RSET (B,B8, .000E+00, .000E+00, .000E+00,
1.047E+00, 3.000E+02, 5.645E+01)
RSET (B,B9, .000E+00, .000E+00, .000E+00,
1.047E+00, 3.000E+02, 5.650E+01)
RSET (B,B10, .000E+00, .000E+00, .000E+00,
1.047E+00, 3.000E+02, 5.700E+01)
RSET (B,B11, .000E+00, .000E+00, .000E+00,
1.047E+00, 3.000E+02, 5.705E+01)
RSET (B,B12, .000E+00, .000E+00, .000E+00,
1.047E+00, 3.000E+02, 5.905E+01)
RSET (B,B13, .000E+00, .000E+00, .000E+00,
1.047E+00, 3.000E+02, 5.995E+01)
RSET (B,B14, .000E+00, .000E+00, .000E+00,
1.047E+00, 3.000E+02, 6.000E+01)
RSET (B,B15, .000E+00, .000E+00, .000E+00,
3.240E-01, 3.000E+02, 8.000E+01)
RSET (B,B16, .000E+00, .000E+00, .000E+00,
3.640E-01, 3.000E+02, 8.000E+01)
RSET (B,B17, .000E+00, .000E+00, .000E+00,
6.440E-01, 3.000E+02, 8.000E+01)
RSET (B,B18, .000E+00, .000E+00, .000E+00,
6.840E-01, 3.000E+02, 8.000E+01)
* Modify default grid
RSET (X,3,3,1.000E+00)
RSET (X,5,2,1.000E+00)
RSET (Y,1,5,1.000E+00)
RSET (Y,3,5,1.000E+00)
RSET (Y,5,5,1.000E+00)
RSET (Y,6,23,1.600E+00)
RSET (Z,1,10,-1.500E+00)
RSET (Z,3,3,1.000E+00)
RSET (Z,5,5,1.000E+00)
RSET (Z,7,5,1.000E+00)
RSET (Z,8,3,1.000E+00)
RSET (Z,10,5,1.500E+00)
* Cylindrical-polar grid
CARTES=F
*****
GROUP 7. Variables stored, solved & named
ONEPHS=T
NAME (14)=TEMP;NAME (16)=OXIG
SOLVE (P1,U1,V1,TEMP,OXIG)
SOLUTN (P1,y,y,y,p,p,p)
STORE (RHO1,VPOR,EPOR,NPOR,HPOR)
GROUP 9. Properties
PRNDTL (TEMP)=8.0;PRNDTL (OXIG)=8.383E-01
HUNIT=1.0/4186.;ENUL=1.0E-06
RHO1=GRND1;RHO1A=1001.3;RHO1B=-0.17428
TURMOD (KEMODL)
GROUP 11. Initialization of variable or porosity fields

```



```

INIADD=F
FIINIT(TEMP)=15.0
conpor(lam1 ,0.00,volume,-#1,-#5,-#1,-#4,-#9,-#9)
conpor(lam2 ,0.00,volume,-#1,-#5,-#4,-#4,-#6,-#8)
conpor(lam3 ,0.00,volume,-#2,-#4,-#5,-#5,-#6,-#6)
conpor(lam4 ,0.00,volume,-#1,-#1,-#4,-#4,-#5,-#5)
conpor(lam5 ,0.00,volume,-#5,-#5,-#4,-#4,-#5,-#5)
conpor(lam6 ,0.00,volume,-#2,-#2,-#4,-#5,-#4,-#5)
conpor(lam7 ,0.00,volume,-#4,-#4,-#4,-#5,-#4,-#5)
conpor(lam8 ,0.00,volume,-#3,-#3,-#4,-#5,-#4,-#4)
conpor(lam9 ,0.00,volume,-#1,-#5,-#4,-#4,-#2,-#3)
conpor(lam10 ,0.00,volume,-#1,-#5,-#2,-#3,-#2,-#2)
conpor(lam11 ,0.00,volume,-#1,-#5,-#2,-#2,-#3,-#7)
patch(TEMPLIN,LINVLZ,1,9,1,40,32,35,1,1)
init(TEMPLIN, temp,0.5263,15.0)
GROUP 13. Boundary conditions and special sources
PATCH(ENTRADA,HIGH, #1,#5,1,5,#3,#3,1,LSTEP)
COVAL(ENTRADA,W1,FIXVAL,GRND)
COVAL(ENTRADA,OXIG,FIXVAL,13.0)
PATCH(SALIDA,HIGH,1,NX,1,NY,NZ,NZ,1,LSTEP)
COVAL(SALIDA,P1,1.0,0.0)
COVAL(SALIDA,TEMP,onlyms,same)
COVAL(SALIDA,OXIG,onlyms,same)
PATCH(BUOYANCY,PHASEM,1,nx,1,ny,1,nz,1,lstep)
COVAL(BUOYANCY,w1,fixflu,grnd1)
PATCH(SUMEO2,NWALL,1,nx,ny,ny,1,nz,1,lstep)
COVAL(SUMEO2,OXIG,1./prndtl(oxig),0.0)
buoya=0.;buoyb=0.0;buoyc=-9.81
conpor(ducto,0.0,volume,-4,-4,-16,-17,-16,-20)
conpor(ducta,0.0,volume,-6,-6,-16,-17,-16,-20)
*** El siguiente parche es para short wave SOLAR RADIATION
PATCH(SOLRAD,FREEVL,1,NX,1,NY,NZ-1,NZ,1,LSTEP)
COVAL(SOLRAD, TEMP,FIXFLU,GRND)
*** El siguiente parche es para SOLAR RADIATION superficial
PATCH(SUPRAD,HIGH,1,NX,1,NY,NZ,NZ,1,LSTEP)
COVAL(SUPRAD, TEMP,FIXFLU,GRND)
*** El siguiente parche es para net ATMOSPHERE RADIATION
PATCH(NETRAD,HIGH,1,NX,1,NY,NZ,NZ,1,LSTEP)
COVAL(NETRAD, TEMP,FIXFLU,NETFLU)
*** El siguiente parche es para long wave BACK RADIATION
PATCH(BACRAD,HIGH,1,NX,1,NY,NZ,NZ,1,LSTEP)
COVAL(BACRAD, TEMP,FIXFLU,GRND)
*** El siguiente parche es para perdidas por EVAPORACION
PATCH(EVAPORA,HIGH,1,NX,1,NY,NZ,NZ,1,LSTEP)
COVAL(EVAPORA, TEMP,FIXFLU,GRND)
*** flotacion para k y epsilon
patch(kebuoy,phasesm,1,nx,1,ny,1,nz,1,lstep)
coval(kebuoy,ke,grnd,grnd)
coval(kebuoy,ep,grnd,grnd)
GROUP 15. Termination of sweeps
lsweep=150
csg1=a;idispa=3
restrt(all)

```

```

relax(temp,falsdt,10.0)
relax(oxig,falsdt,300.0)
relax(u1,falsdt,0.1)
relax(v1,falsdt,0.1)
relax(w1,falsdt,0.1)
relax(ke,falsdt,1.0)
relax(ep,falsdt,1.0)
GROUP 19. Data communicated by satellite to GROUND
    vel. max. en aereador
rg(97)=1.205
    Radio del ducto de entrada
rg(96)=0.7
STOP

```

```

CC*****
SUBROUTINE GROUND
INCLUDE 'ppath/d_earth/SATEAR'
INCLUDE 'ppath/d_earth/GRDLOC'
INCLUDE 'ppath/d_earth/GRDEAR'
EQUIVALENCE (IZ,IZSTEP)
CXXXXXXXXXXXXXXXXXXXXXXXXXXXXXXXXXXXXXXXXXXXXXXXXXXXXX USER SECTION STARTS:
PARAMETER (NPNAM=1000)
PARAMETER (NXDIM=200,NYDIM=100)
DIMENSION DY (NYDIM,NXDIM) ,GRHO (NYDIM,NXDIM) ,GVIST (NYDIM,NXDIM)
DIMENSION GENB (NYDIM,NXDIM) ,GCOE (NYDIM,NXDIM) ,GVAL (NYDIM,NXDIM)
DIMENSION GKE (NYDIM,NXDIM) ,GEP (NYDIM,NXDIM) ,GCO (NYDIM,NXDIM)
DIMENSION GDRHODY (NYDIM,NXDIM) ,GKON (NYDIM,NXDIM)
DIMENSION GTEM (NYDIM,NXDIM) ,GKD (NYDIM,NXDIM) ,GEXP (NYDIM,NXDIM)
DIMENSION GC2 (NYDIM,NXDIM) ,GYCOOR (NYDIM,NXDIM)
DIMENSION GVPOR (NYDIM,NXDIM)
LOGICAL LGCOND,LGTEMP
C*****
C--- GROUP 13. Boundary conditions and special sources
C----- SECTION 1 ----- coefficient = GRND
    IF(NPATCH.EQ.'SOLRAD') THEN
        if(rg(3).gt.0.0) then
            call fn1(co,2.0E-10)
        else
            call fn1(co,0.0)
        endif
    ENDIF
c@v--- Calculate k-eps buoyancy source terms
    IF(NPATCH.EQ.'KEBUOY') CALL GRKEBY
    RETURN
131 CONTINUE
C----- SECTION 12 ----- value = GRND
CVOR..Fuente para SHORT WAVE SOLAR RADIATION (volumetrica)
C.....RG(1)=eta;RG(2)=beta;RG(3)=FI(radiacion)
    IF(NPATCH.EQ.'SOLRAD') THEN
        call fn1(grsp1,0.0)
        call fn0(grsp2,yg2d)
        call fn25(grsp2,-1.0)
        call fn33(grsp2,yvlast)

```

```

        call fn36(grsp1,grsp2,rg(1)*(1.0-rg(2))*rg(3),-rg(1))
        call fn0(val,grsp1)
        call fn25(val,rg(99)*0.5E+10)
        if(rg(3).eq.0.0) call fn25(val,0.0)
c        if(isweep.eq.lisweep) call prn('SHRT',val)
        ELSE IF(NPATCH.EQ.'BACRAD') THEN
CVOR..Fuente para LONG WAVE BACK RADIATION (superficial)
C.....RG(4)=a;RG(5)=b
        call fn2(val,14,rg(4),rg(5))
        call fn25(val,-rg(99))
        call fn26(val,vpor)
c        if(isweep.eq.lisweep) call prn('LONG',val)
CVOR...Calculos para la SOLAR RADIATION superficial
        ELSE IF(NPATCH.EQ.'SUPRAD') THEN
        call fn1(val,rg(2)*rg(3)*rg(99))
capp cambiar el fn26 de abajo por un fn2
        call fn26(val,vpor)
        ELSE IF(NPATCH.EQ.'NETRAD') THEN
        GCNET1=208.733
        GCNET2=6.2363
        GCLD=0.05
        GNETFLU=(GCNET1+GCNET2*RG(14))*(1.0+0.17*GCLD**2.0)*RG(99)
        call fn1(val,GNETFLU)
        call fn26(val,vpor)
        ELSE IF(NPATCH.EQ.'EVAPORA') THEN
CVOR..Fuente para perdidas por EVAPORACION (superficial)
C.....RG(6)=FISUP;RG(7)=FI2M;RG(8)=PBAR;RG(9)=W2M
C.....RG(10)=C1;RG(11)=C2;RG(12)=C3;RG(13)=ALFA;RG(14)=TAIRE
        LGCOND=.false.
        LGTEMP=.false.
        call getyx(h1,gtem,nydim,nxdim)
        call getyx(val,gval,nydim,nxdim)
        do jx=ixf,ixl
        do jy=iyf,iyl
            psatw=rg(13)*exp(rg(10)+rg(11)/(gtem(jy,jx)+273.15)+
&            rg(12)*alog(gtem(jy,jx)+273.15))
            pvapw=rg(6)*psatw
            omegaw=0.622*pvapw/(rg(8)-pvapw)
            thetavw=(gtem(jy,jx)+273.15)*(1.0+0.61*omegaw)
            GTSV=thetavw-273.15
            thetava=(rg(14)+273.15)*(1.0+0.61*omegaa)
            GTAV=thetava-273.15
            delpav=pvapw-pvapa
            if(delpav.lt.0) then
c                write(6,*) 'Pvapw menor que pvapaire '
                LGCOND=.true.
                delpav=0.0
            endif
            deltats=GTSV-GTAV
            if(deltats.lt.0) then
                LGTEMP=.true.
c                write(6,*) 'TSagua menor que TSaire'
                deltats=0.0

```

```

endif
GQEVFREE=2.7*deltats**(1.0/3.0)*deltapv
GQEVFORC=3.2*abs(rg(9))*deltapv
GQEVAPO=SQRT(GQEVFREE*GQEVFREE+GQEVFORC*GQEVFORC)
CVOR..Termino adicional para perdidas CONVECTIVAS
IF(LGCOND.or.LGTEMP) THEN
  GRB=0.0
  GO TO 763
ENDIF
GRB=6.19E-04*rg(8)*(gtem(jy,jx)-rg(14))/deltapv
763  gval(jy,jx)=-GQEVAPO*(1.0+GRB)*rg(99)
    end do
    end do
    call setyx(val,gval,nydim,nxdim)
    call fn26(val,vpor)
  ENDF
c@v--- Calculate k-eps buoyancy source terms
IF(NPATCH.EQ.'KEBUOY') CALL GRKEBY
RETURN
1312 CONTINUE

C--- GROUP 19. Special calls to GROUND from EARTH
C * ----- SECTION 1 ---- Start of time step.
CJDY ** Calculos para el valor de TAIRE, FI(radiacion), W2M, **
IF(lg(14)) THEN
cerr  IF(ISWEEP.GE.1.OR.(ISTEP.EQ.1.AND.ISWEEP.EQ.0)) THEN
      IF(TIM.LE.30.0*86400.0) THEN
        rg(14) = 0.06453/86400.0*TIM+11.868
        rg(17) = rg(14)-2.0
        rg(3) = 105.0*sin(3.141593*(TIM+20.0*86400.0)
&          / (380.0*86400.0))+130.0
        rg(9) = 2.1
        rg(7) = 0.085*cos((TIM+120*86400)*3.141593/
&          (180*86400))+0.415
        rg(16) = GCD*GRAIRE*ABS(RG(9))*RG(9)
.....
.....  and so on
.....
      ELSEIF(TIM.GT.330.0*86400.0.AND.TIM.LE.360.0*86400.0)
THEN
        rg(14) = -0.064250/86400.0*TIM+35.2310
        rg(17) = rg(14)-2.0
        rg(3) = 105.0*sin(3.141593*(TIM+20.0*86400.0)
&          / (380.0*86400.0))+130.0
        rg(9) = 2.3
        rg(7) = 0.085*cos((TIM-240*86400)*3.141593/
&          (180*86400))+0.415
        rg(16) = GCD*GRAIRE*ABS(RG(9))*RG(9)
      ENDF
    ENDF
    RETURN
192 CONTINUE
C*****

```



```

      GKECON=1.0
      ELSE IF (INDVAR.EQ.EP) THEN
        GKECON=C3E
      ENDIF
      CALL GETYX (GRSP5, GGENB, NYDIM, NXDIM)
      CALL GETYX (KE, GKE, NYDIM, NXDIM)
      CALL GETYX (CO, GCOE, NYDIM, NXDIM)
      DO JX = 1, NX
      DO JY = 1, NY
        GENBKE=GGENB (JY, JX)
        IF (GENBKE.LE.0.0) THEN
          GCOE (JY, JX)=-GKECON*GENBKE/ (GKE (JY, JX) +1.E-20)
        ELSE
          GCOE (JY, JX)=1.0E-10
        ENDIF
      END DO
      END DO
      CALL SETYX (CO, GCOE, NYDIM, NXDIM)
      ELSE IF (ISC.EQ.12) THEN
        IF (INDVAR.EQ.KE) THEN
          CALL FN1 (GRSP6, 1.0)
        ELSE IF (INDVAR.EQ.EP) THEN
          CALL FN15 (GRSP6, EP, KE, 0.0, C3E)
        ENDIF
      CALL GETYX (VAL, GVAL, NYDIM, NXDIM)
      CALL GETYX (GRSP5, GGENB, NYDIM, NXDIM)
      CALL GETYX (KE, GKE, NYDIM, NXDIM)
      CALL GETYX (GRSP6, GKON, NYDIM, NXDIM)
      DO JX = 1, NX
      DO JY = 1, NY
        GENBKE=GGENB (JY, JX)
        IF (GENBKE.LE.0.0) THEN
          GVAL (JY, JX)=0.0
        ELSE
          GVAL (JY, JX)=1.E+10*GENBKE*GKON (JY, JX)
        ENDIF
      END DO
      END DO
      CALL SETYX (VAL, GVAL, NYDIM, NXDIM)
      ENDIF
      RETURN
      END

```